Electronic Supporting Information for:

Ligand-Triplet Migration in Iridium(III) Cyclometalates Featuring π-Conjugated Isocyanide Ligands

Joseph M Favale Jr., Cory E. Hauke, Evgeny O. Danilov, James E. Yarnell, and Felix N. Castellano*

Department of Chemistry, North Carolina State University (NCSU), Raleigh, NC, 27695-8204, United States

EMAIL ADDRESS: fncastel@ncsu.edu

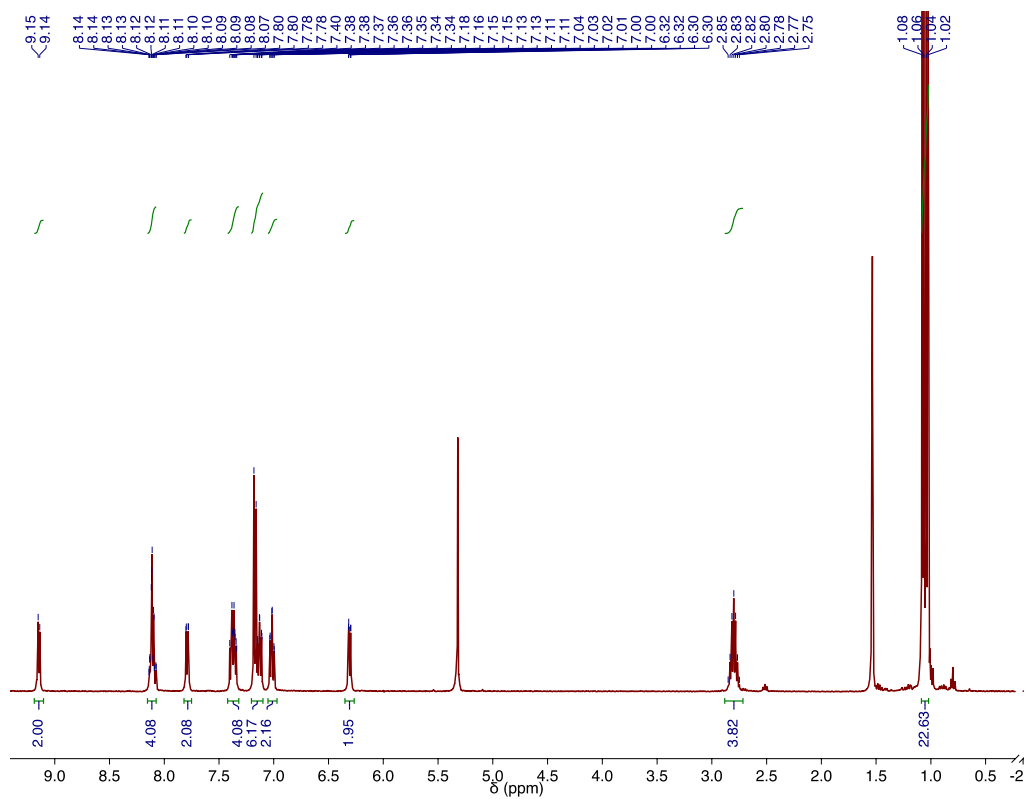* To whom correspondence should be addressed. Phone: (419) 372-7513 Fax: (419) 372-9809

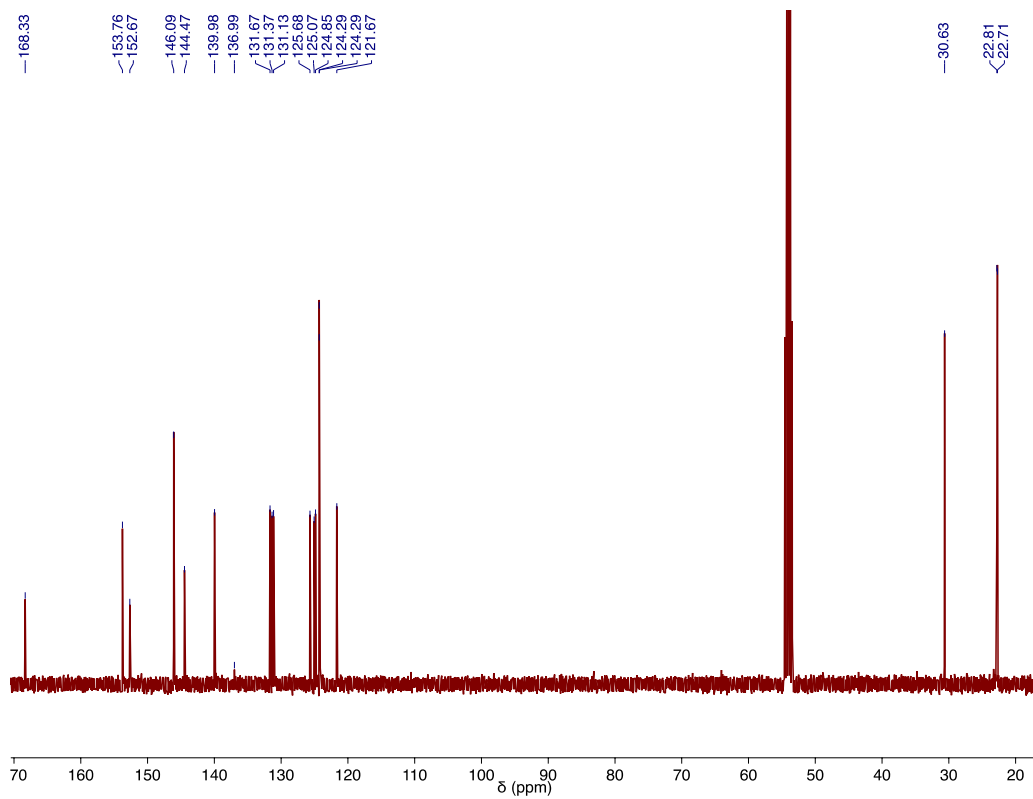**Figure S1:** ^1H NMR spectrum of **1** in CD_2Cl_2 (400 MHz).

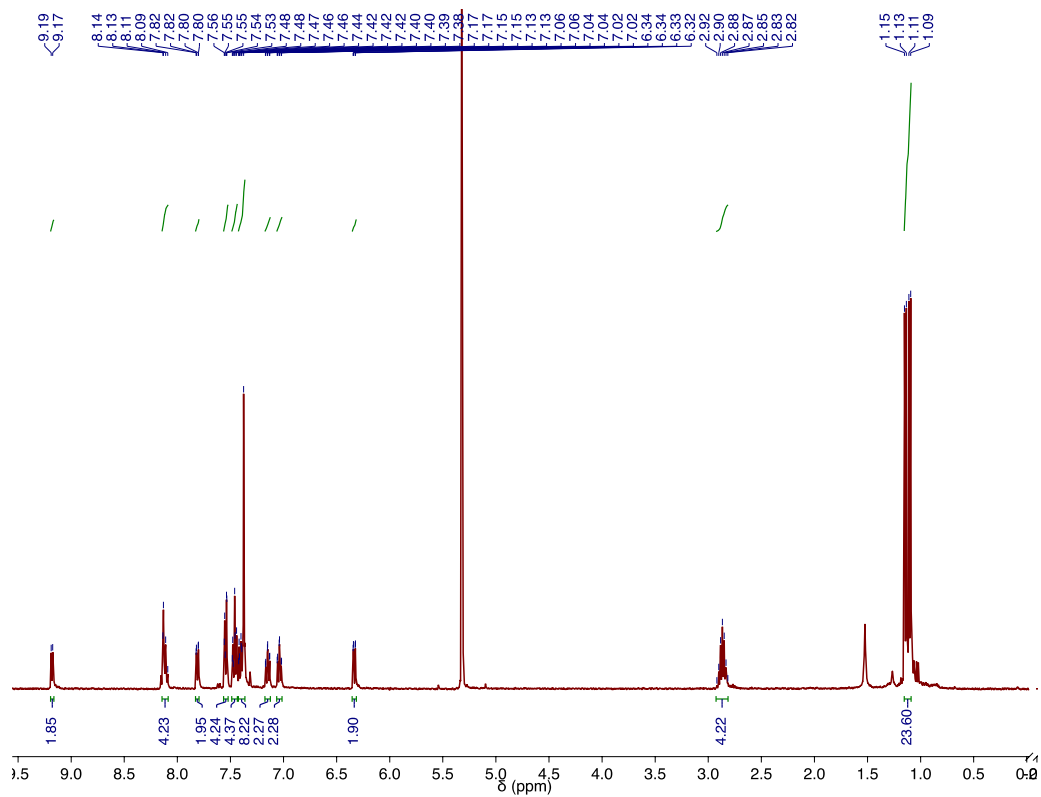**Figure S2:** ^{13}C NMR spectrum of **1** in CD_2Cl_2 (100 MHz).

Figure S3: ^{1}H NMR spectrum of **2** in CD_2Cl_2 (400 MHz).
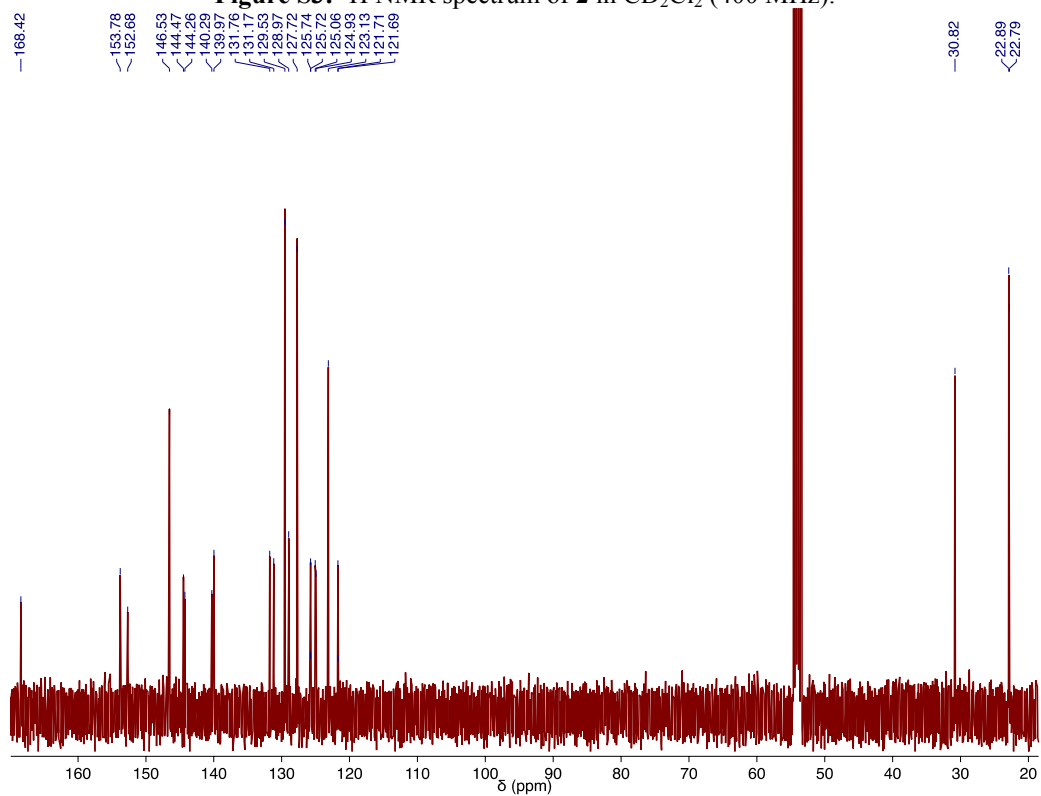

Figure S4: ^{13}C NMR spectrum of **2** in CD_2Cl_2 (100 MHz).
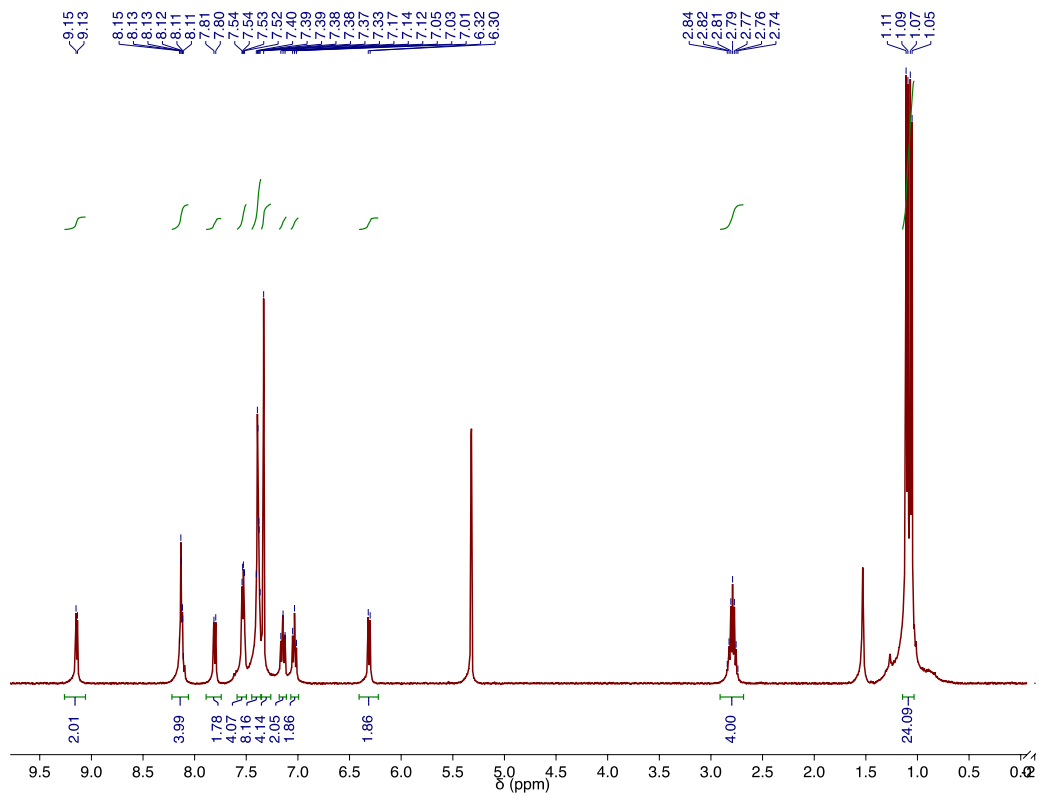
Figure S5: ^{1}H NMR spectrum of **3** in CD_2Cl_2 (400 MHz).
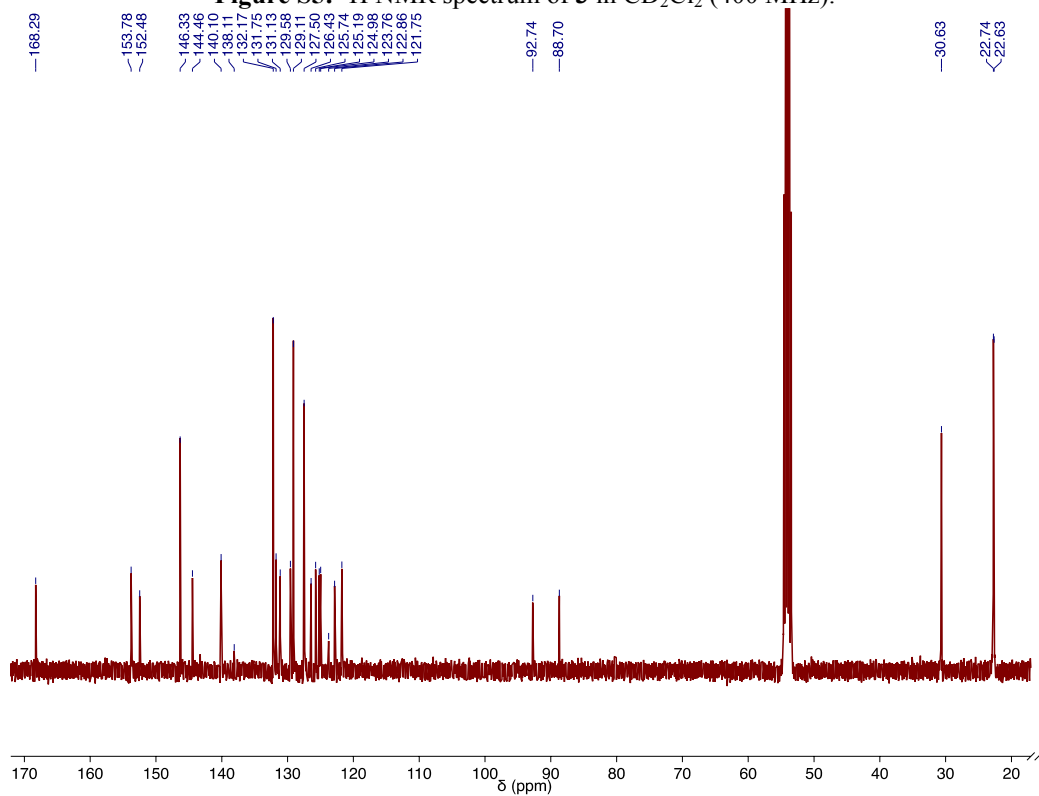

Figure S6: ^{13}C NMR spectrum of **3** in CD_2Cl_2 (100 MHz).
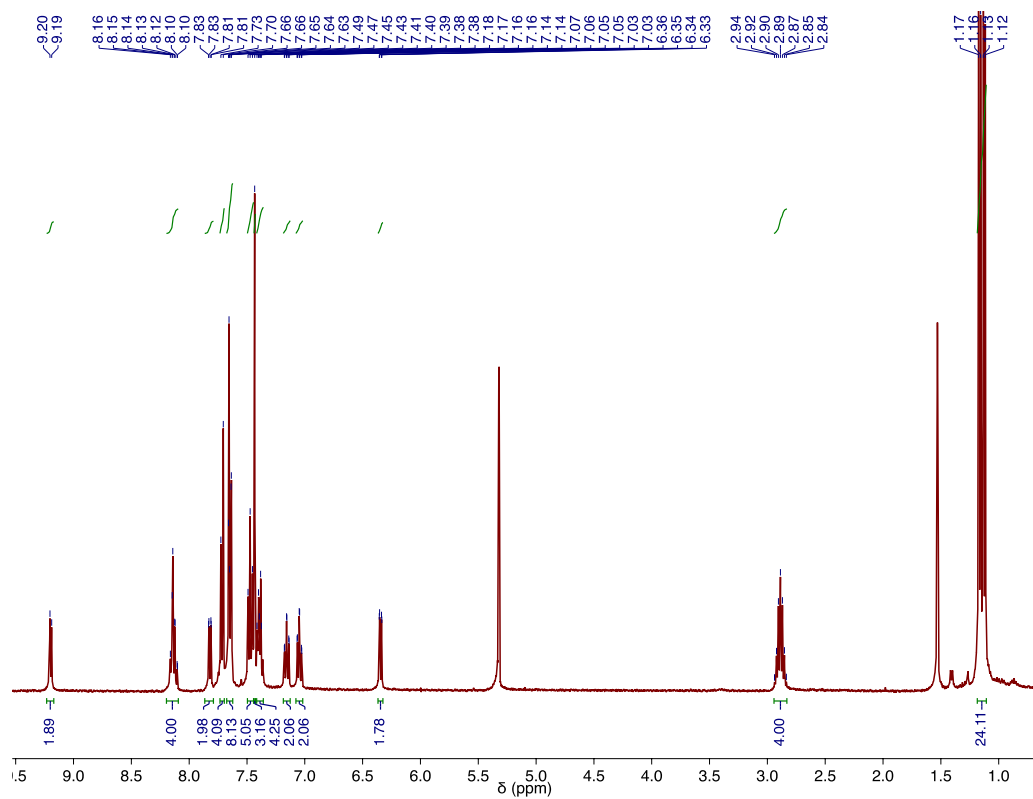
Figure S7: ^{1}H NMR spectrum of **4** in CD_2Cl_2 (400 MHz).
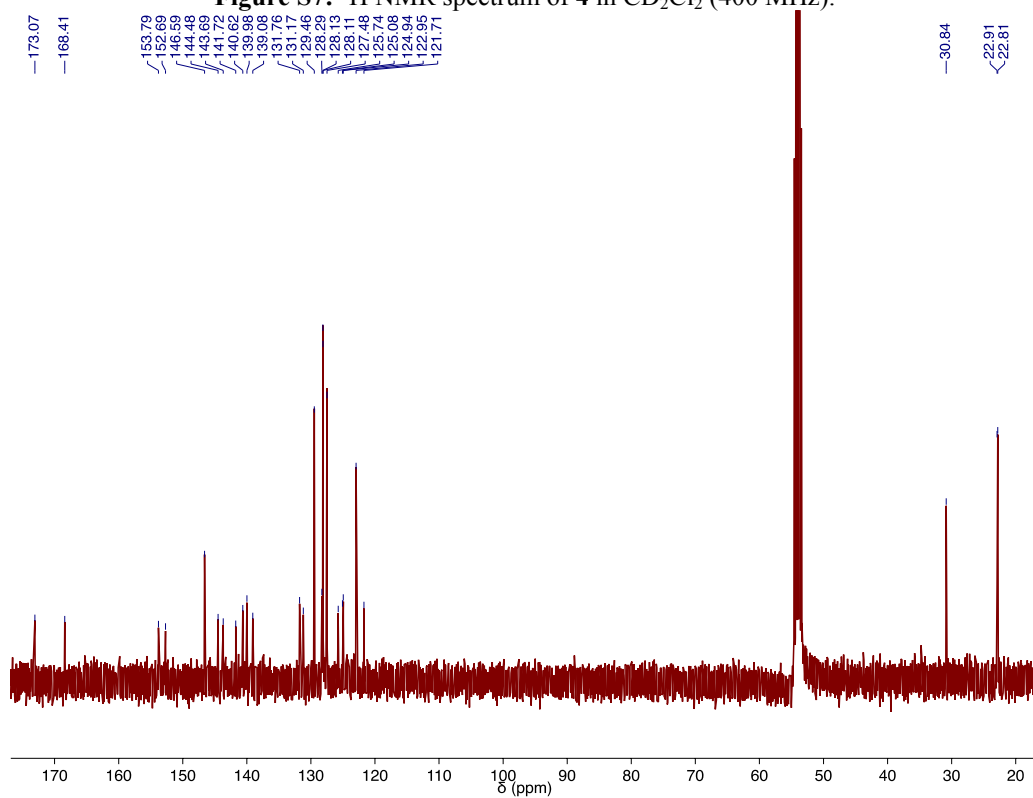

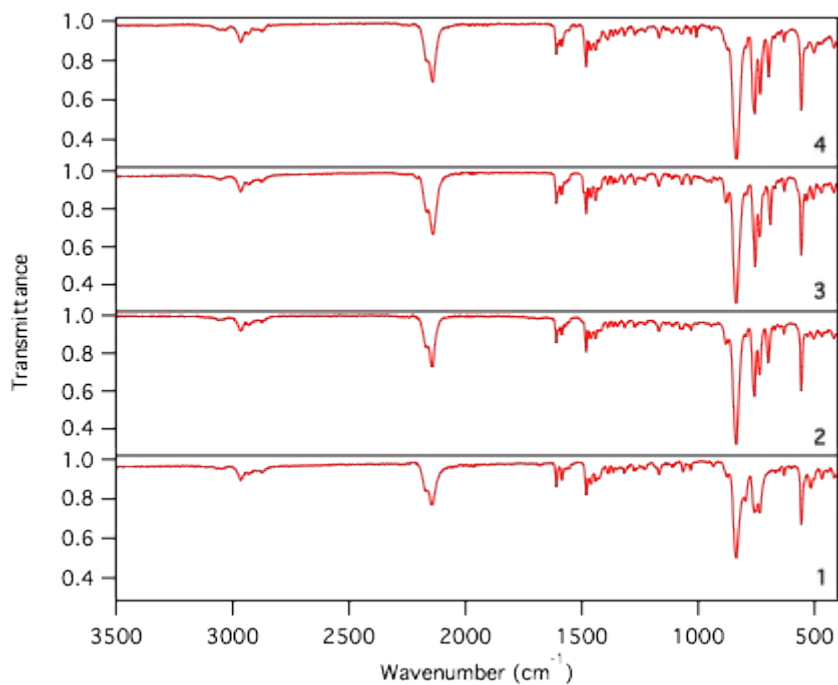**Figure S8:** ^{13}C NMR spectrum of **4** in CD_2Cl_2 (100 MHz).

Figure S9: FTIR-ATR spectra of **1-4** as powders.

Figure S10: ns-TA difference spectra of **1-4** in THF. Spectra recorded using 355 nm excitation for all samples.

Figure S11: ns-TA kinetic decays of **1**–**4** in THF demonstrating single-exponential fits (blue). ns-TA kinetics recording of most prominent transient signals in each with 355 nm excitation for all samples. Sample of **3** measured at concentration of ~1.6 ×10⁻⁶ M. Sample of **4** measured at concentration of ~2.5 ×10⁻⁶ M.

Figure S12: Ultrafast TA kinetics of **1** in THF measured to 250 ps.

Figure S13: Ultrafast TA kinetics of **1** in THF measured to 20 ps.

Figure S14: Ultrafast TA kinetics of **2** in THF measured to 60 ps.

Figure S15: Ultrafast TA kinetics of **2** in THF measured across the complete time window (6 ns).

Figure S16: Ultrafast TA kinetics of **3** in THF measured across the complete time window (6 ns).

Figure S17: Ultrafast TA kinetics of **3** in THF measured to 60 ps.

S10

Figure S18: Ultrafast TA kinetics (at 571 nm) of **4** in THF measured to 60 ps.
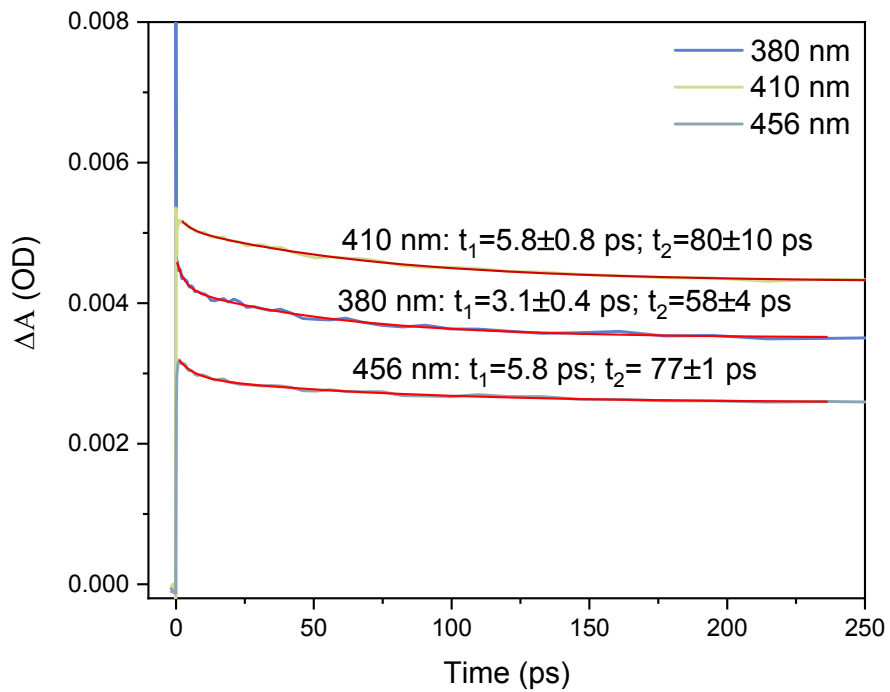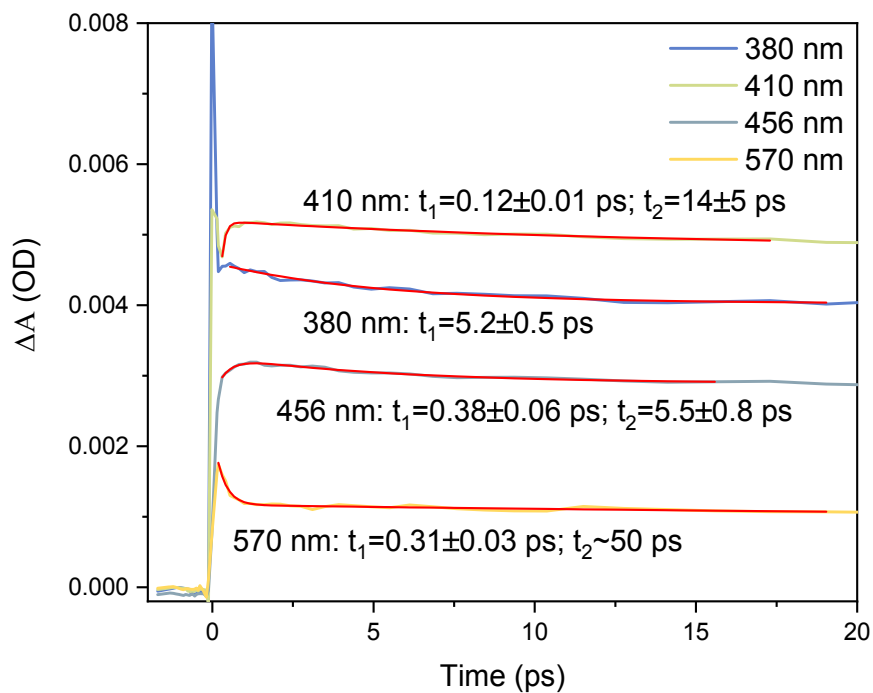

Figure S19: Ultrafast TA kinetics of **4** in THF measured to 10 ps.

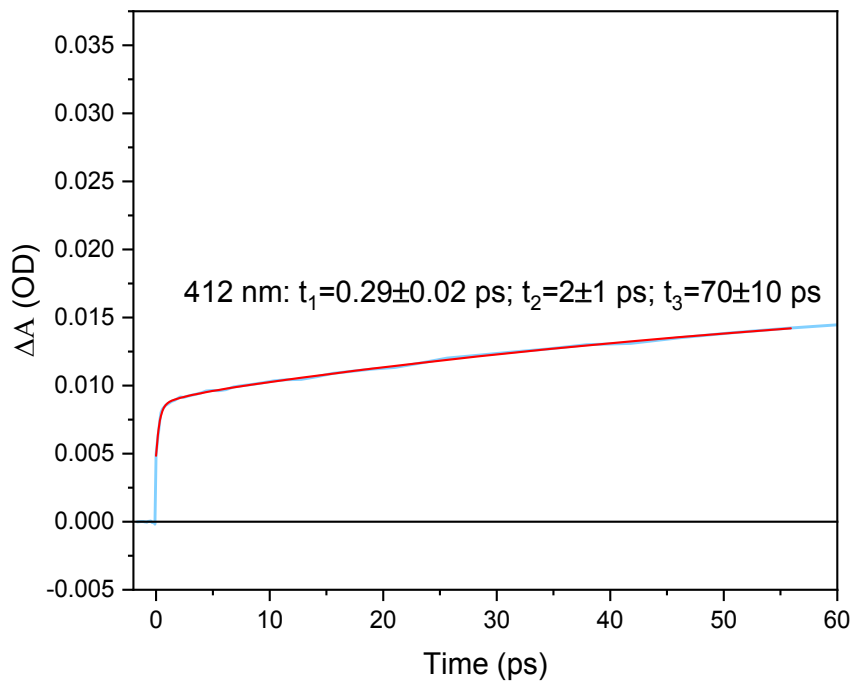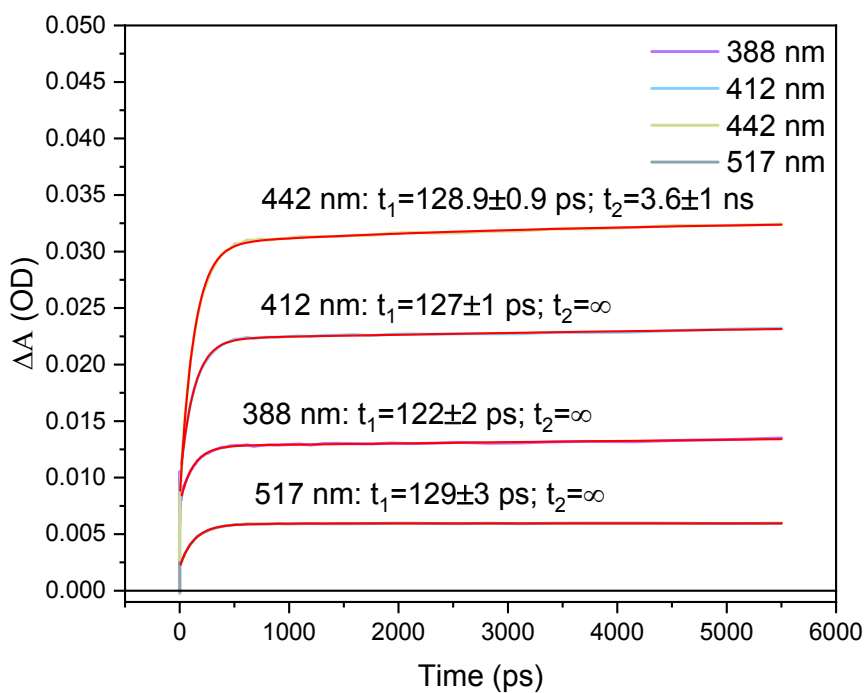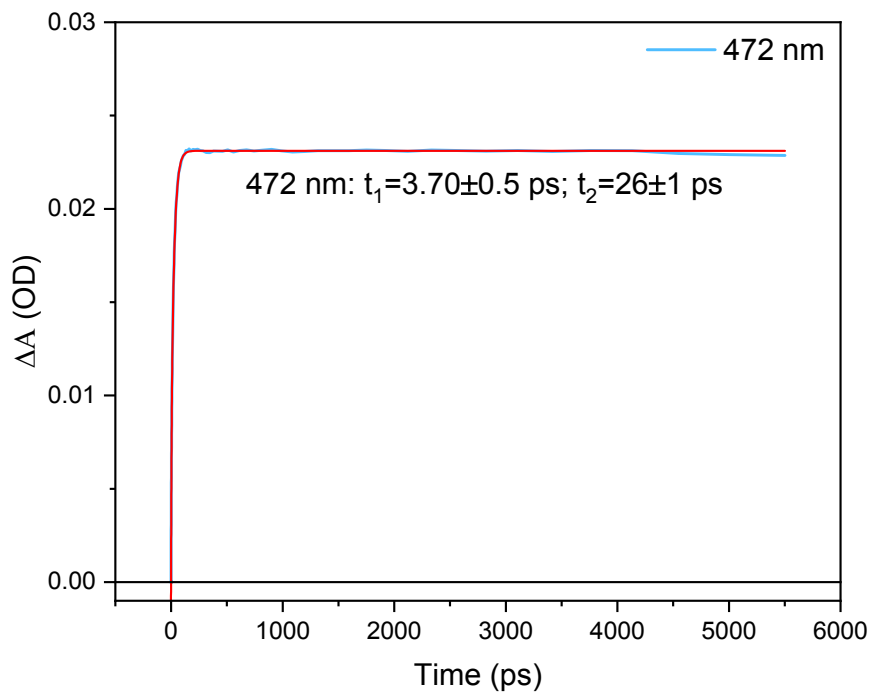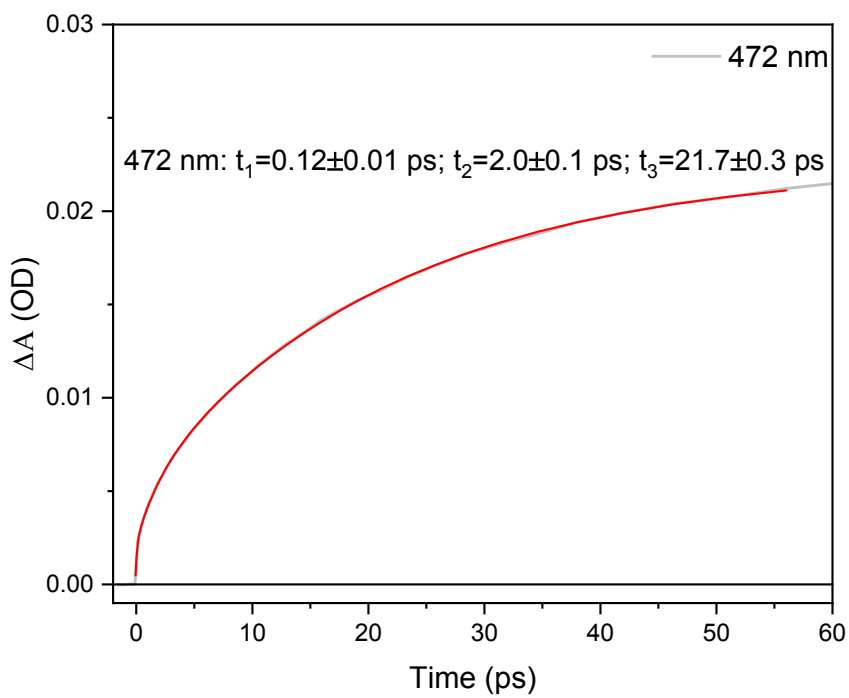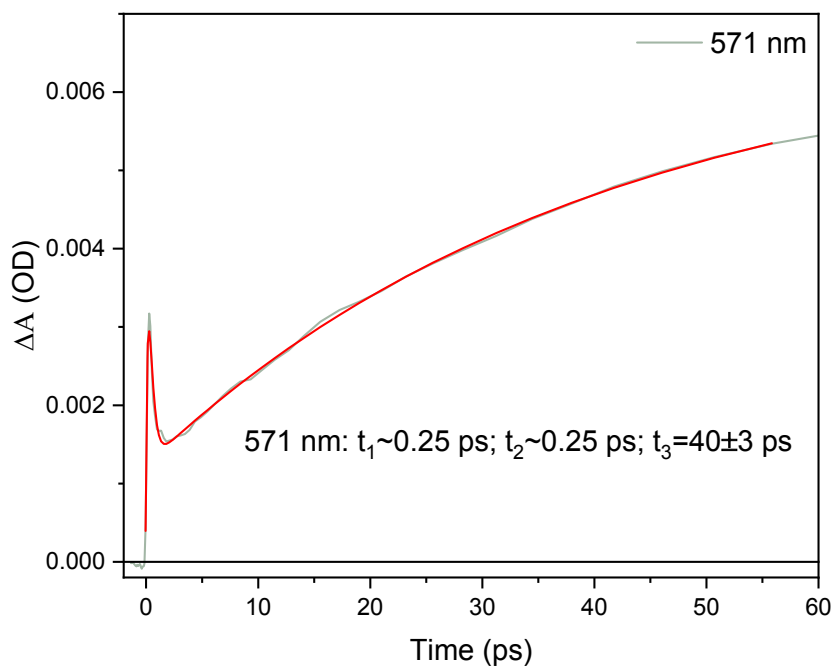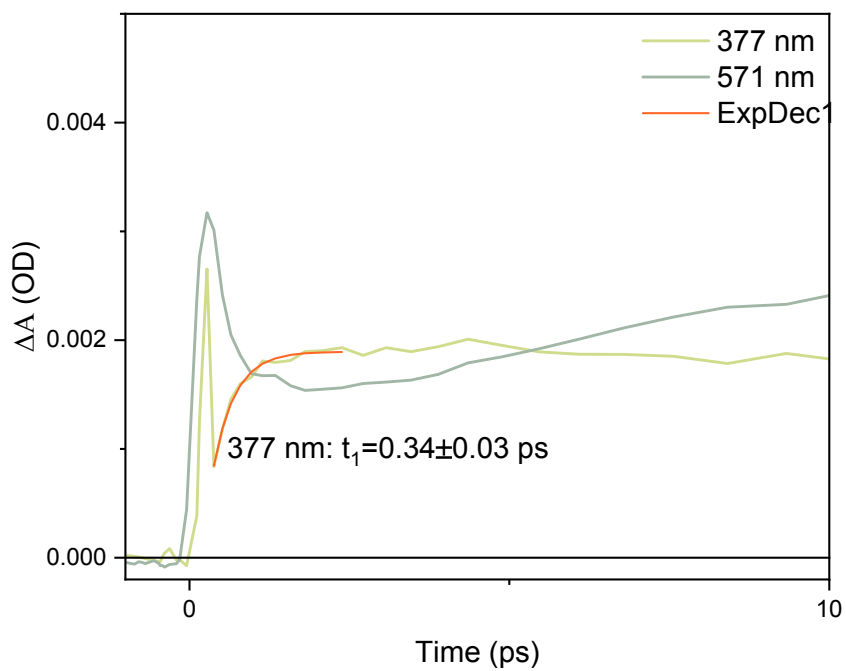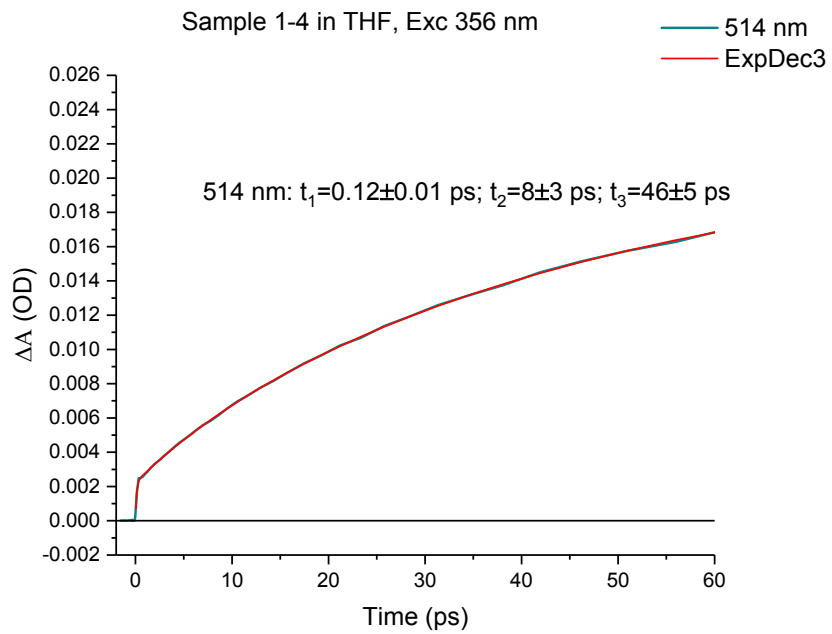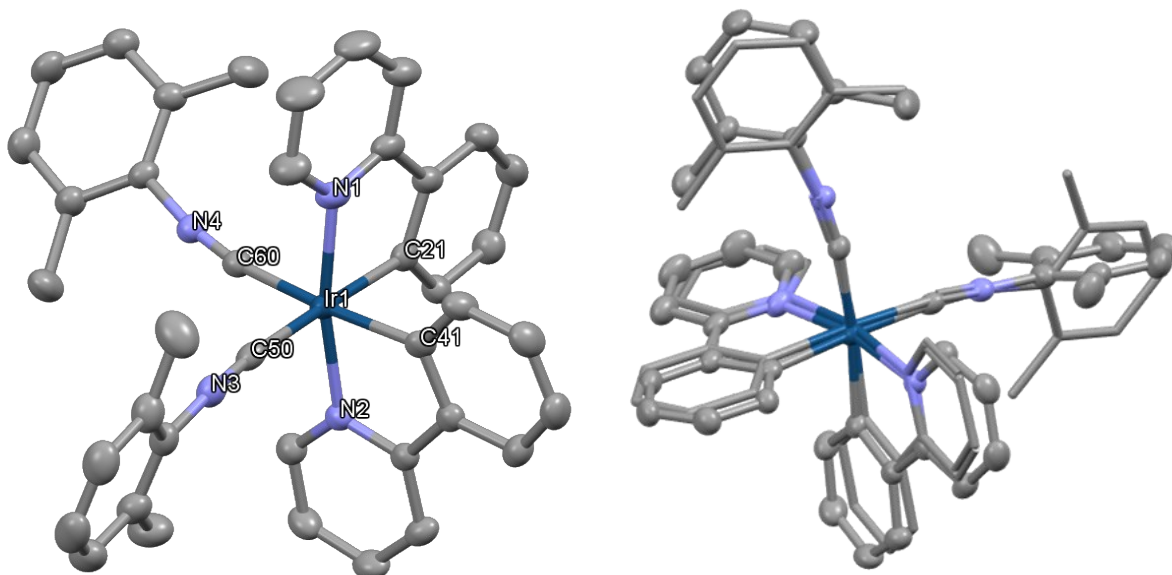**Figure S20:** Ultrafast TA kinetics of **4** in THF measured to 600 ps.

Figure S21. Crystal structure of [Ir(ppy)$_2$(dmpCN)$_2$]$^+$ published previously in *Inorg. Chem.* **2016**, *55*, 2299−2308 (left), and overlay of crystal structure to optimized geometry at the M06/Def2-SVP/SDD level of theory (right).

Table S1. Comparison of optimized geometries using different hybrid functionals to the crystal structure [Ir(ppy)$_2$(dmpCN)$_2$]$^+$ from *Inorg. Chem.* **2016**, *55*, 2299−2308.

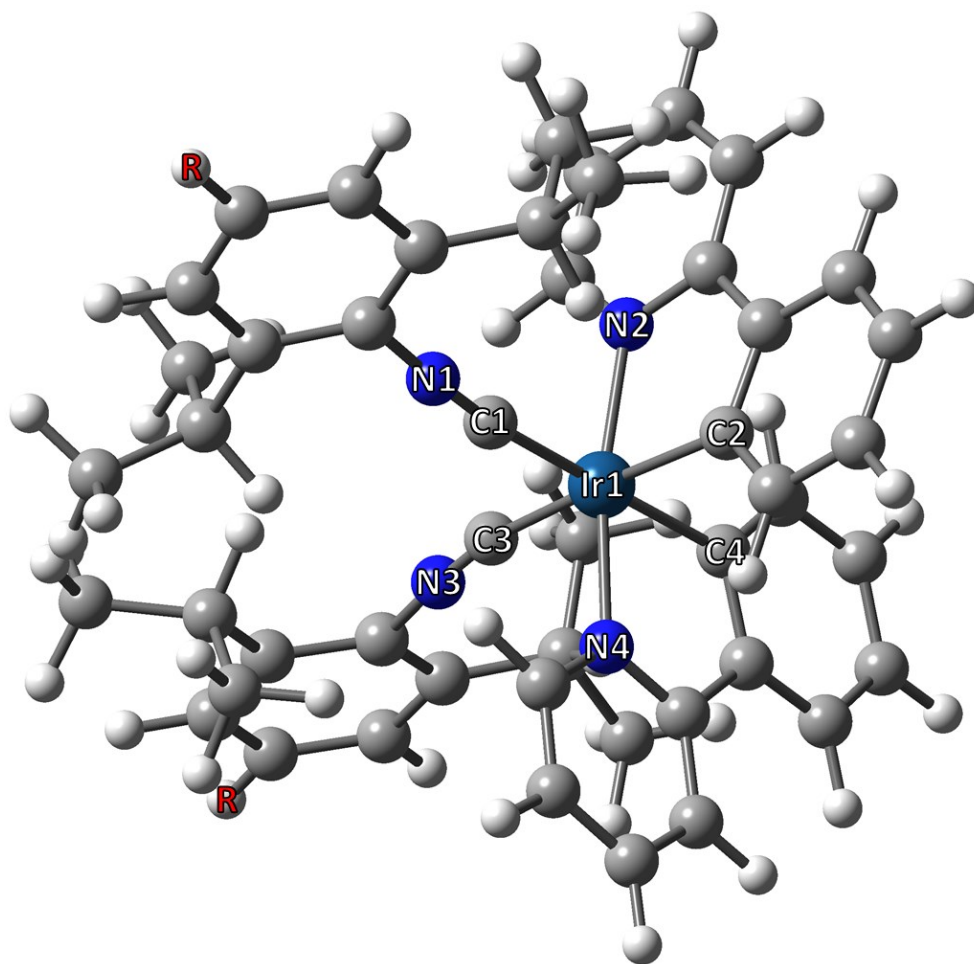|		Crystal Structure	M06/Def2-SVP/SDD	B3LYP/Def2-SVP/SDD	PBE0/Def2-SVP/SDD
Bond Length (Å)	**Ir1-C60**	2.023(3)	2.0471	2.0512	2.0202
	N4-C60	1.151(4)	1.1724	1.1728	1.1708
	Ir1-N1	2.060(3)	2.0922	2.1030	2.0764
	Ir1-C21	2.052(4)	2.0725	2.0851	2.0659
	Ir1–C50	2.012(4)	2.0455	2.0512	2.0202
	N3–C50	1.155(5)	1.1724	1.1728	1.1708
	Ir1-N2	2.061(3)	2.0915	2.1030	2.0764
	Ir1-C41	2.048(3)	2.0721	2.0851	2.0659
Bond Angle (deg)	**C60-Ir1-C50**	95.22(14)	98.97	96.19	96.88
	Ir1-C60-N4	169.8(3)	173.17	175.64	175.52
	Ir1-C50-N3	173.8(3)	172.08	175.63	175.52
Molecular Overlay (Å)	**RMSD**	---	0.9573	1.0197	1.0439
	Max. D	---	3.0118	2.9481	3.2894

Figure S22. General molecular structure of the molecules in this study.

Table S2. Comparison of optimized geometries of the complexes in this study.

		1	2	3	4
Bond Length (Å)	**Ir1–C1**	2.034	2.035	2.035	2.037
	N1–C1	1.171	1.171	1.171	1.171
	Ir1-N2	2.090	2.091	2.092	2.092
	Ir1-C2	2.072	2.074	2.075	2.074
	Ir1-C3	2.041	2.041	2.037	2.037
	N3-C3	1.171	1.171	1.172	1.171
	Ir1-N4	2.091	2.090	2.091	2.092
	Ir1-C4	2.075	2.072	2.074	2.074
Bond Angle (deg)	**C1-Ir1-C3**	97.39	97.06	96.81	96.22
	Ir1-C1-N1	173.95	173.74	173.20	175.12
	Ir1-C3-N3	170.03	171.60	174.75	175.10

Table S3. Select frontier molecular orbital energies (eV) as determined at the PCM/M06/Def2-SVP/SDD level of theory.

	1	2	3	4
LUMO+3	-1.776	-1.993	-2.174	-2.073
LUMO+2	-1.898	-2.094	-2.247	-2.172
LUMO+1	-2.176	-2.177	-2.343	-2.176
LUMO	-2.247	-2.247	-2.418	-2.252
HOMO	-6.933	-6.895	-6.726	-6.648
HOMO-1	-7.111	-6.958	-6.731	-6.655
HOMO-2	-7.399	-7.014	-6.975	-6.949
HOMO-3	-7.424	-7.127	-7.133	-7.112

Figure S23. Frontier orbital diagram constructed for **1**. Calculations performed at DFT//PCM/M06/Def2-SVP/SDD level of theory.

Figure S24. Frontier orbital diagram constructed for **2**. Calculations performed at DFT//PCM/M06/Def2-SVP/SDD level of theory.
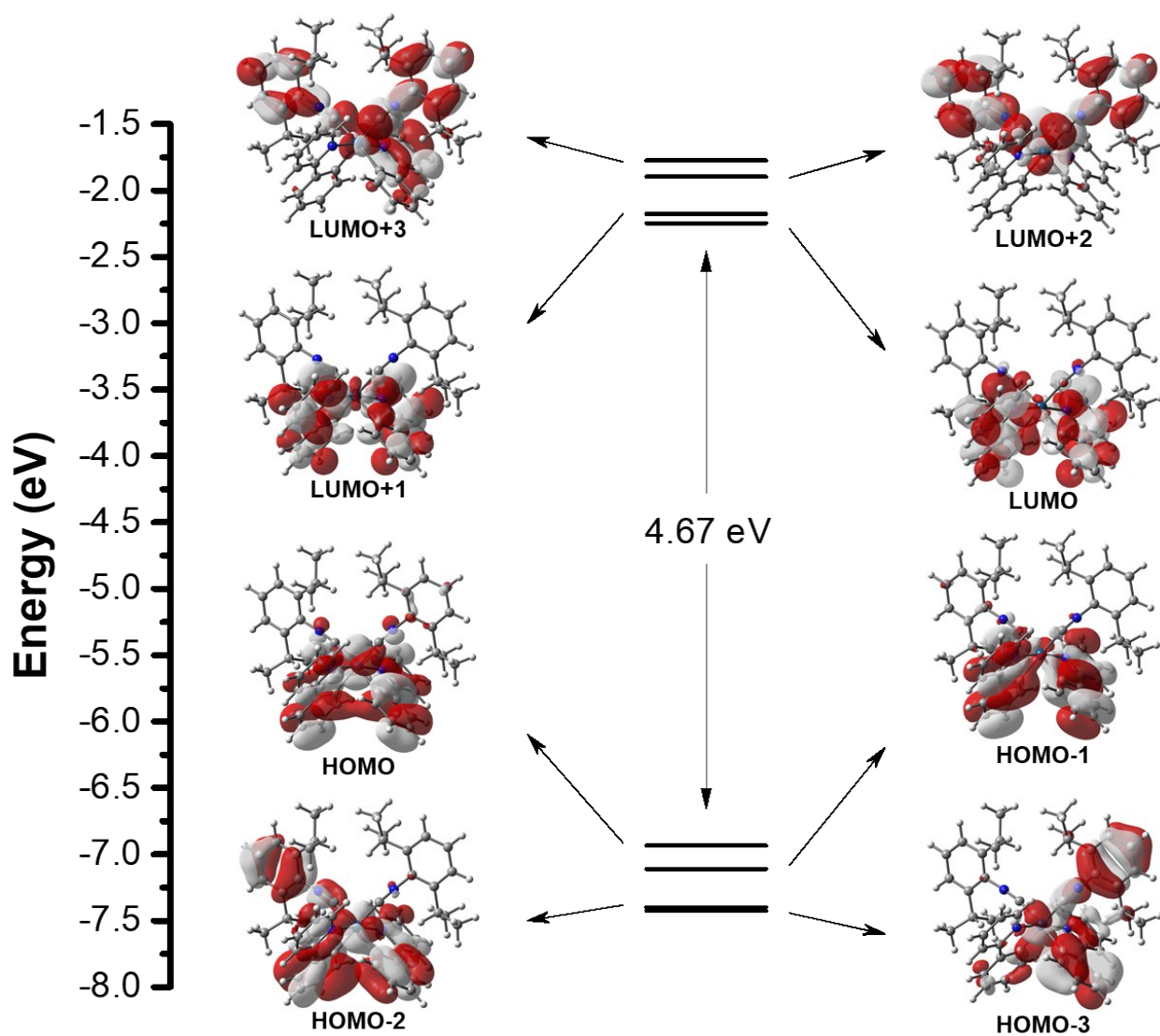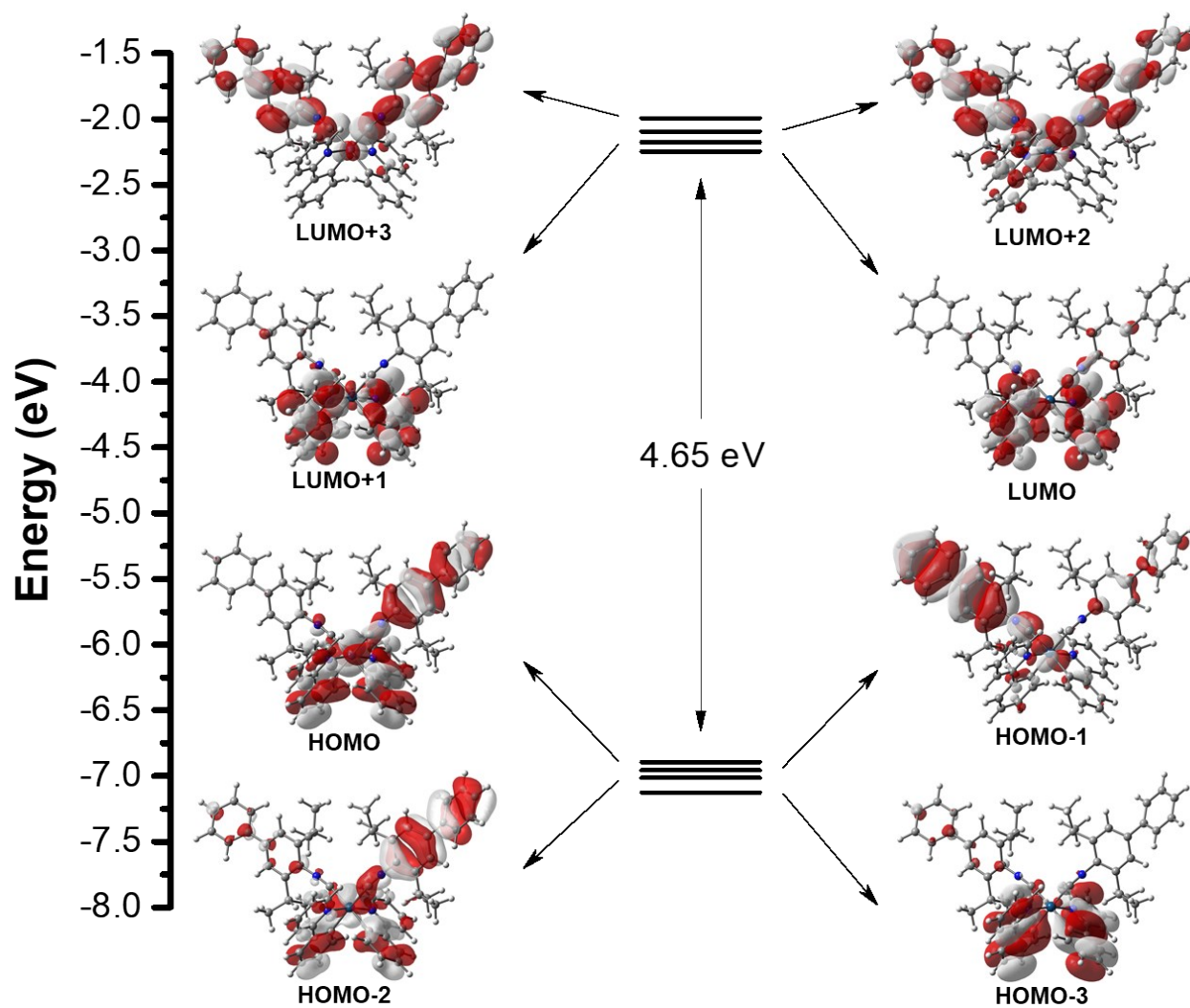
Figure S25. Frontier orbital diagram constructed for **3**. Calculations performed at DFT//PCM/M06/Def2-SVP/SDD level of theory.

Figure S26. Frontier orbital diagram constructed for **4**. Calculations performed at DFT//PCM/M06/Def2-SVP/SDD level of theory.
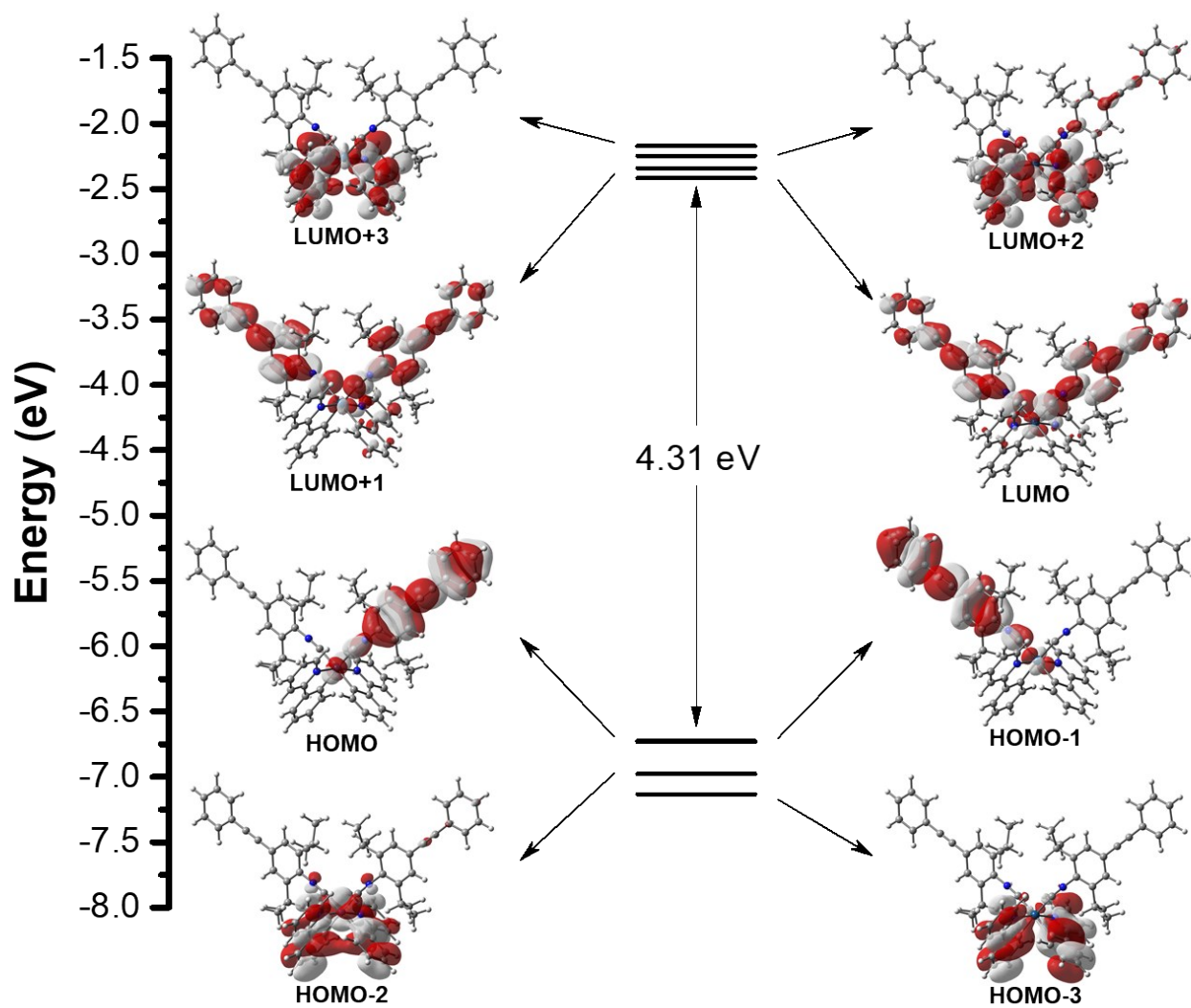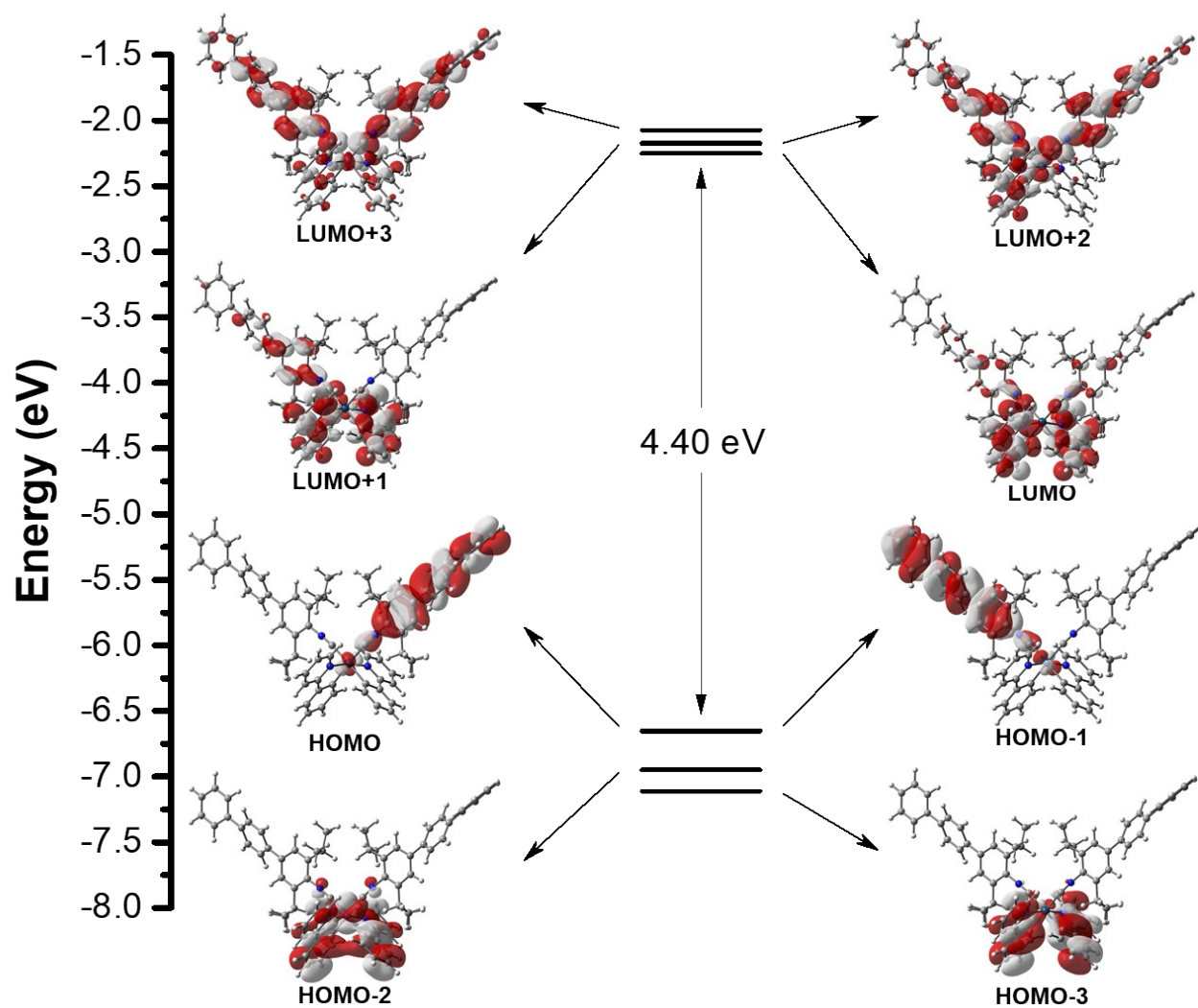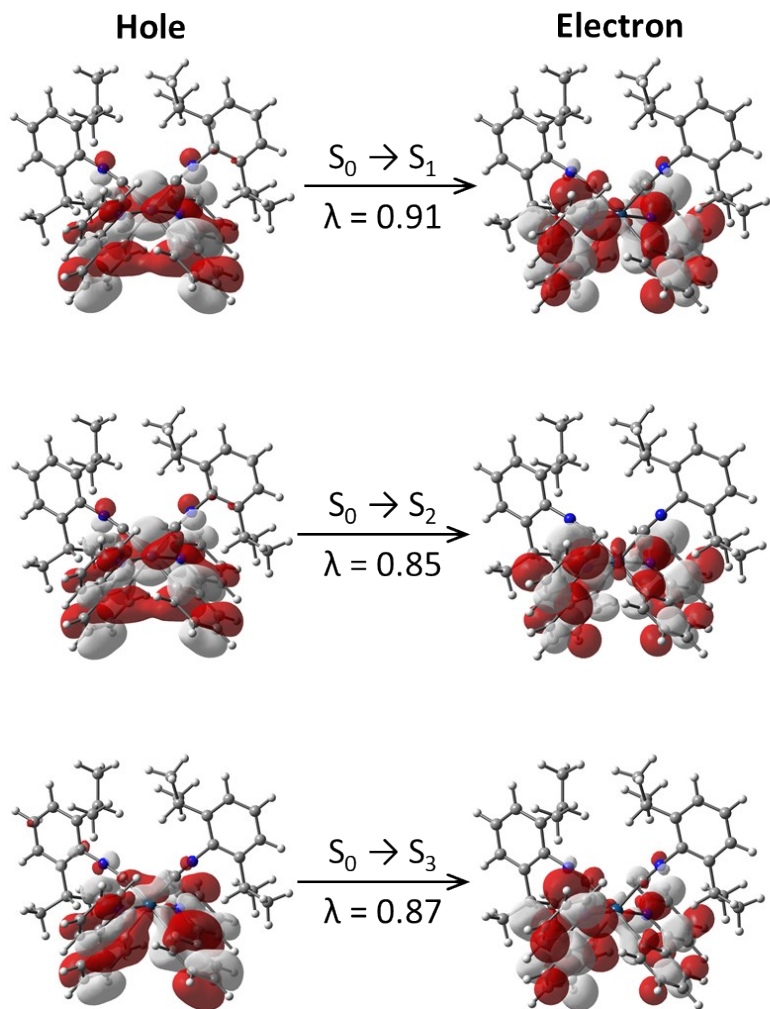
Table S4. Wavelength, energies, and oscillator strength (*f*) for selected $S_0 \leftarrow S_n$ excitations as determined via TDDFT at the PCM/M06/Def2-SVP/SDD level of theory. Experimental UV/Vis data obtained in tetrahydrofuran at room temperature.

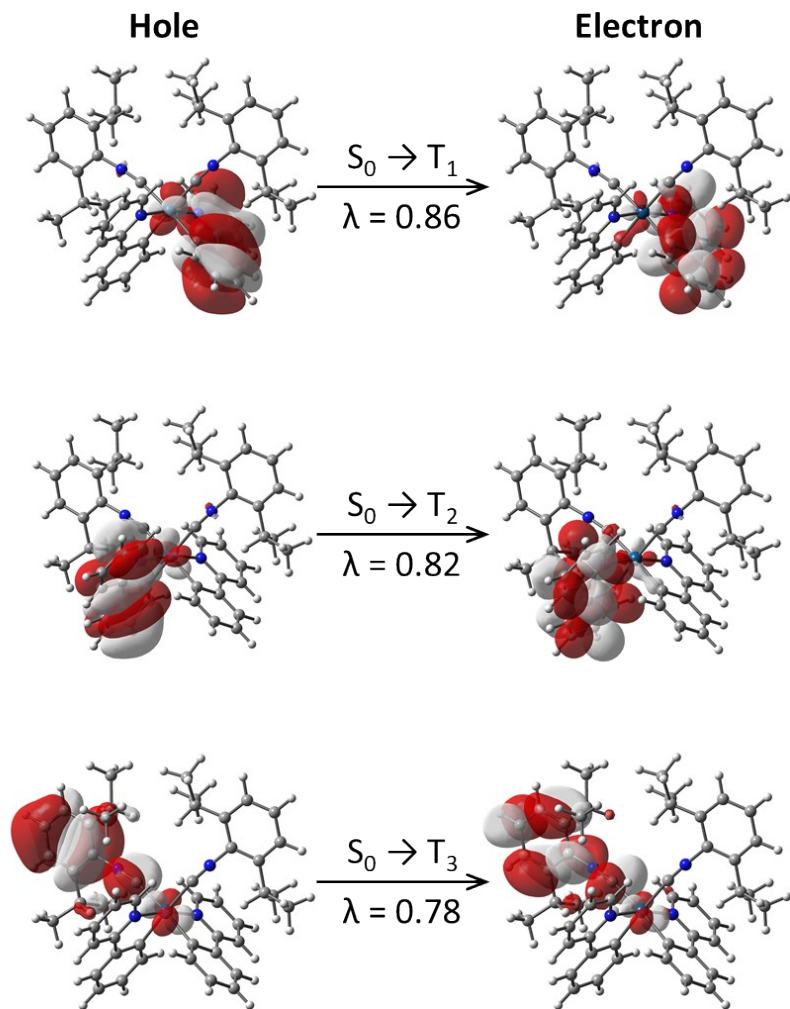| Molecules	$\lambda_{abs\ max}$ /nm, eV (ε/M^{-1} cm^{-1})	$S_0 \leftarrow S_1$ /nm, eV (*f*) $S_0 \leftarrow S_2$ /nm, eV (*f*) $S_0 \leftarrow S_3$ /nm, eV (*f*)	$S_0 \leftarrow T_1$ /nm, eV $S_0 \leftarrow T_2$ /nm, eV $S_0 \leftarrow T_3$ /nm, eV
1	346, 3.58 (8500)	335, 3.70 (0.1281) 330, 3.76 (0.0115) 310, 4.00 (0.0281)	433, 2.86 433, 2.87 385, 3.22
2	346, 3.58 (7900)	335, 3.70 (0.1227) 330, 3.76 (0.0060) 315, 3.94 (1.0445)	434, 2.86 434, 2.86 433, 2.86
3	352, 3.52 (8300)	355, 3.49 (2.2984) 346, 3.58 (1.0607) 334, 3.71 (0.1596)	506, 2.45 506, 2.45 433, 4.33
4	312, 3.97 (107400)	339, 3.66 (2.0607) 333, 3.72 (0.2719) 332, 3.73 (0.9950)	460, 2.69 459, 2.70 432, 2.87

Figure S27. Natural transition orbitals (NTOs) for select $S_0 \rightarrow S_n$ excitations (left) and select $S_0 \rightarrow T_n$ excitations (right) of **1** determined at the TD-DFT//PCM/M06/Def2-SVP/SDD level of theory. λ is the fraction of the hole−particle contribution to the excitation.
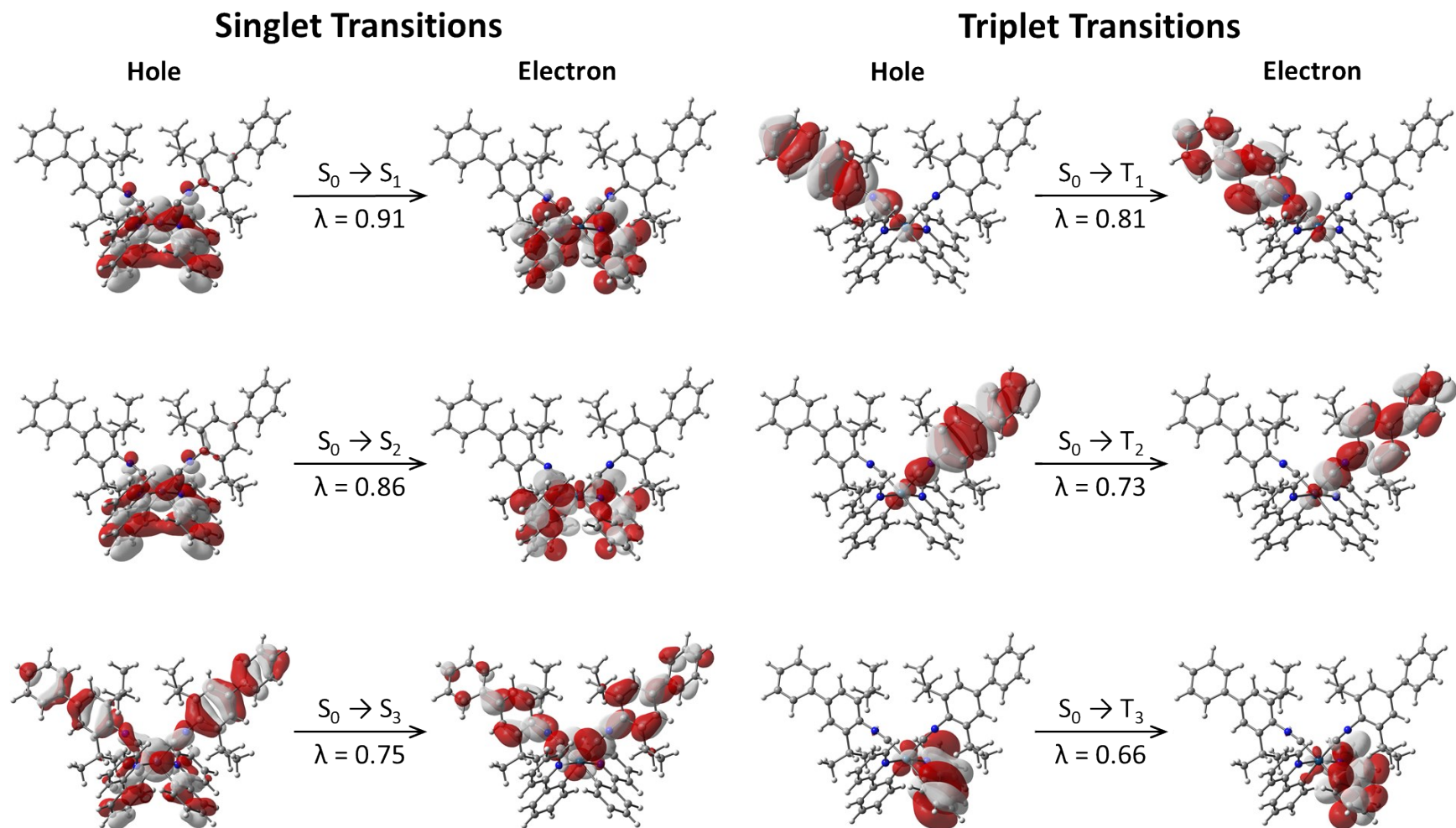
Figure S28. Natural transition orbitals (NTOs) for select $S_0 \rightarrow S_n$ excitations (left) and select $S_0 \rightarrow T_n$ excitations (right) of **2** determined at the TD-DFT//PCM/M06/Def2-SVP/SDD level of theory. λ is the fraction of the hole−particle contribution to the excitation.
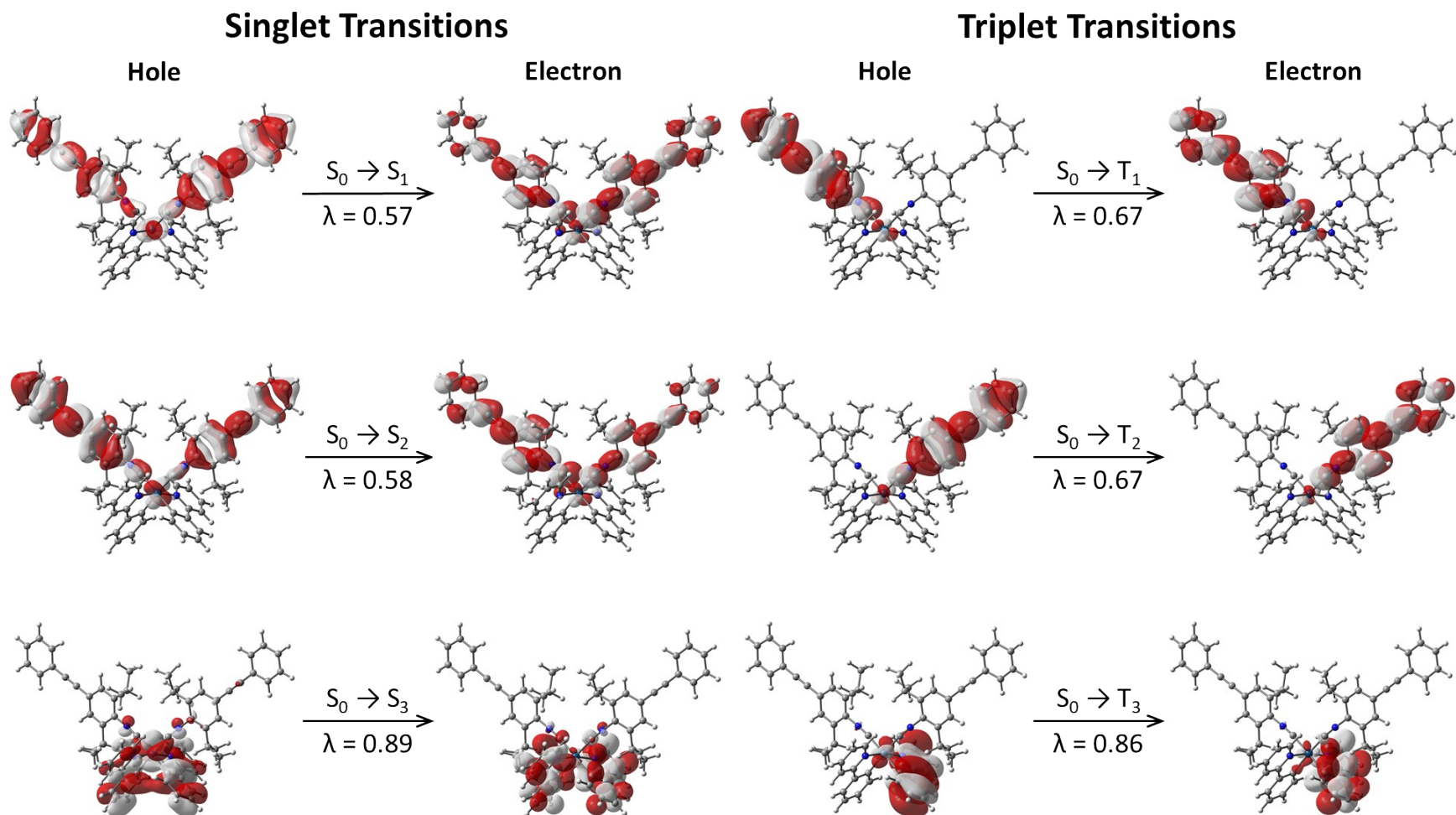
Figure S29. Natural transition orbitals (NTOs) for select $S_0 \rightarrow S_n$ excitations (left) and select $S_0 \rightarrow T_n$ excitations (right) of **3** determined at the TD-DFT//PCM/M06/Def2-SVP/SDD level of theory. λ is the fraction of the hole−particle contribution to the excitation.
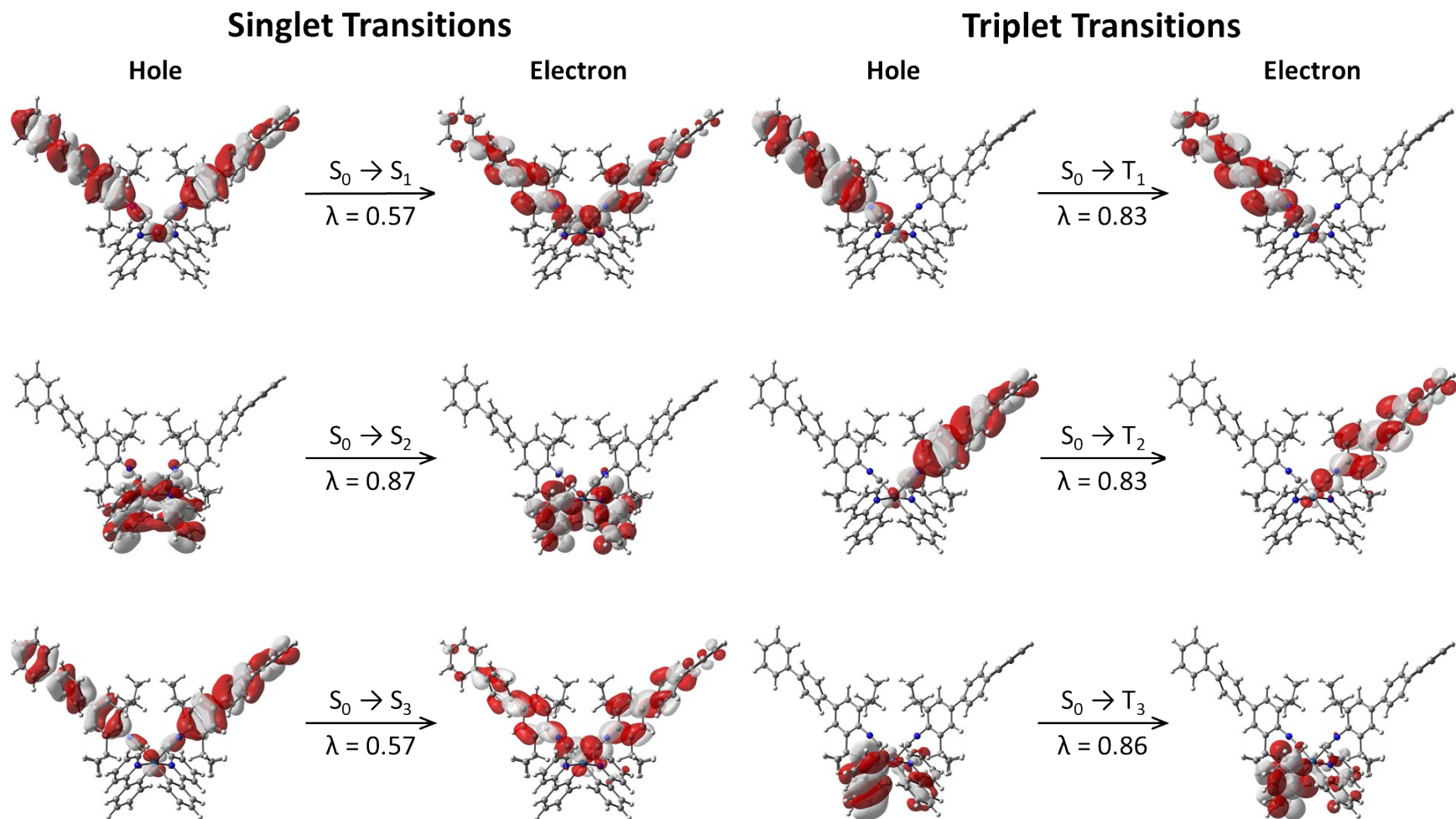
Figure S30. Natural transition orbitals (NTOs) for select $S_0 \rightarrow S_n$ excitations (left) and select $S_0 \rightarrow T_n$ excitations (right) of **4** determined at the TD-DFT//PCM/M06/Def2-SVP/SDD level of theory. λ is the fraction of the hole–particle contribution to the excitation.